J. Plasma Phys. (2022), *vol*. 88, 905880513
Published by Cambridge University Press
doi:10.1017/S0022377822001039

Momentum transfer and plasma rotation caused by destabilized eigenmodes in tokamaks

Ya.I. Kolesnichenko [1],†, Hyun-Tae Kim [2], V.V. Lutsenko [1], A.V. Tykhyy [1], R.B. White [3], Yu.V. Yakovenko [1] and JET contributors

[1]Institute for Nuclear Research, Prospekt Nauky 47, Kyiv 03028, Ukraine

[2]United Kingdom Atomic Energy Authority, Culham Science Centre, Abingdon OX14 3DB, UK

[3]Princeton Plasma Physics Laboratory, Princeton, NJ 08543, USA

(Received 16 June 2022; revised 28 September 2022; accepted 29 September 2022)

The influence of magnetohydrodynamic eigenmodes destabilized by energetic ions on the momentum of these ions and concomitant sheared plasma rotation are studied. Two mechanisms affecting rotation are revealed: (i) spatial channelling (SC) – radially separated emission and absorption of the momentum; (ii) mode induced redistribution (MIR) across the magnetic field of the momentum of energetic ions. Forces arising during SC and MIR produce both toroidal and poloidal rotations. In addition, the momentum emission during SC leads to a radial flux of fast ions and generation of a radial electric field. Using the developed theory, estimates were made for the ITER (International Thermonuclear Experimental Reactor) 15 MA baseline scenario. They show that a global toroidicity-induced Alfvén eigenmode destabilized by alpha particles and neutral beam injection can result in significant radial electric field and forces applied to plasma. However, available data are not sufficient for a reliable prediction of the effects of SC and MIR in ITER. In general, one can expect that sheared rotation arising after destabilization of Alfvén modes and fast magnetoacoustic modes by energetic ions will tend to suppress the turbulence and improve plasma performance. The importance of plasma rotation is supported, in particular, by the fact that during the JET DTE1 experimental campaign the best parameters were achieved in a deuterium–tritium discharge where the rotation frequency was largest.

Key words: plasma waves, fusion plasma, plasma instabilities

1. Introduction

In 2010 it was recognized that destabilized Alfvénic modes can transfer the energy of energetic ions across the magnetic field without producing anomalous heat diffusivity, just because the unstable region does not coincide with the region of the mode damping (Kolesnichenko, Yakovenko & Lutsenko 2010*a*; Kolesnichenko *et al.* 2010*b*). This phenomenon was named ‘spatial channelling’ (SC), see recent work (Kolesnichenko, Tykhyy & White 2020) which includes an overview of various manifestations of SC and relevant references.

† Email address for correspondence: ykoles@ukr.net

When the unstable region is located in the middle of the mode but the mode is damped in the inner and outer regions, both inward and outward energy fluxes are generated: the former at smaller radii, the latter at larger radii. When the unstable region is located at the plasma periphery but the damping region is in the plasma core, inward SC takes place, and the instability heats the plasma core. However, even in this case a considerable outward flux may also be generated in the peripheral region of the mode when the instability growth rate is sufficiently large (Kolesnichenko & Tykhyy 2018).

Presumably, the SC with outward energy flux took place in the NSTX (National Spherical Torus Experiment) experiments described in Stutman *et al.* (2009). In these experiments the increase of neutral beam injection (NBI) power by a factor of three was accompanied with the growth of Alfvénic activity but did not increase the plasma temperature near the magnetic axis. The outward energy channelling could be responsible for this (Kolesnichenko *et al.* 2010*a*,*b*; Belova *et al.* 2017), although there was also an alternative explanation of these experiments that an anomalous diffusivity was generated by multiple modes (Gorelenkov *et al.* 2010). On the other hand, according to Kolesnichenko *et al.* (2018), inward SC of alpha-particle energy by fast magnetoacoustic modes (FMM, known also as CAE) with frequencies either above or approximately the ion gyrofrequency may have played a role in the improved confinement and anomalous ion heating, which seems took place in JET DTE1 experiments with deuterium–tritium (D–T) plasmas (Thomas *et al.* 1998; Thomas 2001; Weisen *et al.* 2014).

The SC leads to radial transfer of not only the energy but also the momentum.

The momentum SC could be another mechanism favourable for plasma confinement in the mentioned DTE1 experiments: the momentum transfer leads to sheared plasma rotation, tending to suppress turbulence in the region of mode location. As will be shown in this work by analysing JET DTE1 data, the best parameters were achieved in the discharge where plasma rotation frequency was highest (D–T discharge #42847). The toroidicity-induced Alfvén eigenmode (TAE) activity was absent in these experiments, only ion cyclotron emission (ICE) which presumably is associated with FMM was observed. This may support the assumption made in Kolesnichenko *et al.* (2018) that FMM could be responsible for the SC (the structure of modes leading to ICE was not measured), although other modes, such as global Alfvén eigenmodes (known as GAE), could lead to plasma rotation.

Note that there are a number of experiments confirming improved plasma characteristics in rotating plasmas. In particular, high fusion performance at high T_i/T_e in JET-ILW baseline plasmas with high NBI heating power was observed, which correlated with high rotation frequency (Kim *et al.* 2018). Correlation between high rotation frequency and confinement was also observed in the DIII-D tokamak; furthermore, it was found in super H-mode experiments that high rotation, not high pedestal, plays the essential role in achieving very high confinement (Ding *et al.* 2020).

Thus, the influence of destabilized eigenmodes on the transverse momentum transfer and concomitant plasma rotation is an important topic. To study this issue is the purpose of this work.

We have to note that energetic ions can affect plasma rotation and its performance through mechanisms which differ from those considered in our work. In particular, they can suppress plasma turbulence, leading to so-called fast ion-induced anomalous transport barrier (known as F-ATB) (Siena *et al.* 2021). Nonlinear evolution of TAE modes can result in generation of zonal flows (Todo, Berk & Breizman 2010).

The work has the following structure. At the beginning, in § 2, the JET database of the DTE1 campaign is analysed in order to compare the plasma rotation velocities in discharges heated by NBI, ion cyclotron resonance heating (ICRH) and fusion produced

https://doi.org/10.1017/S0022377822001039 Published online by Cambridge University Press

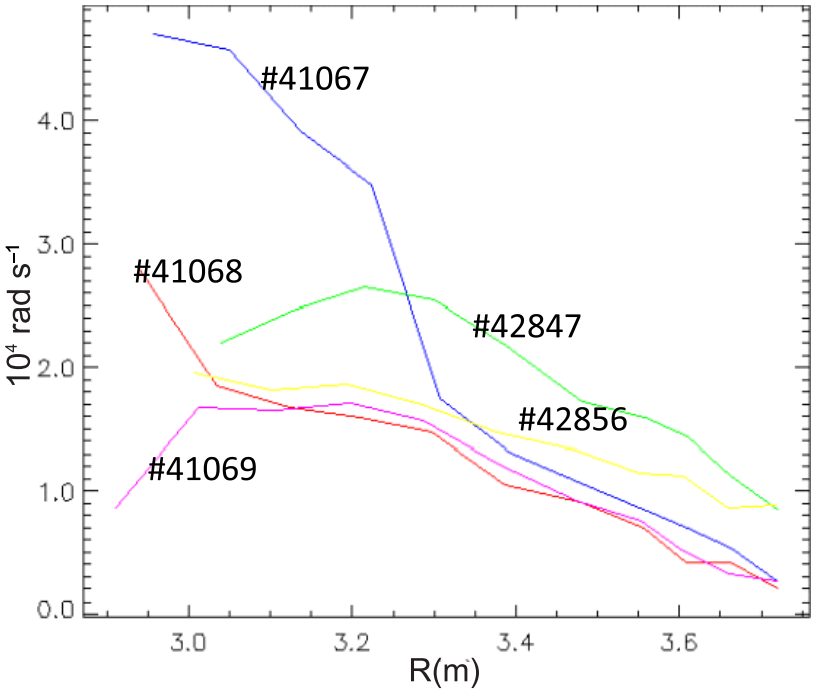

FIGURE 1. Radial dependence of rotation frequency in the JET DTE1 deuterium discharges (#41067, #41068, #41069) and D–T discharges (#42847, #42856). Time evolution of these discharges for 52–55 s was considered (see also Kolesnichenko *et al.* 2018), it clearly shows that the improved performance (i.e. high Ti thereby high fusion performance) is associated with the high rotation frequency.

alpha particles. A theory of the influence of destabilized modes on the momentum of fast-ion population is developed in § 3. At the beginning of this section, a qualitative analysis based on a quantum mechanics analogy is carried out; after that, an approach employing a quasilinear equation for distribution function of fast ions is used. An alternative approach based on a Hamiltonian of a single particle in the presence of a wave is used in Appendix A. Plasma rotation and generation of the radial electric field caused by particle radial fluxes during SC are considered in § 4. The developed theory is applied to ITER (International Thermonuclear Experimental Reactor) in § 5 where effects of a destabilized TAE mode are evaluated. Section 6 summarizes the results obtained in the work. Some peculiarities of plasma rotation in tokamaks are described in Appendix B.

2. Evidence of enhanced plasma rotation in JET DTE1 experiments with improved plasma performance

We selected the same JET discharges of the first deuterium–tritium-experiment campaign (DTE1) which were analysed in Kolesnichenko *et al.* (2018) (see also Thomas *et al.* 1998; Thomas 2001; Weisen *et al.* 2014). They have two important features. First, the overall confinement time was slightly higher at the largest fusion power in D–T experiments. Second, the central ion temperature in D–T discharges was higher than that in deuterium discharges where the ICRH was applied with the heating power approximately that of alpha particles (fusion products) in DT discharges. These facts indicated the

https://doi.org/10.1017/S0022377822001039 Published online by Cambridge University Press

presence of some anomalous heating mechanism because mainly electrons are heated during slowing down of 3.5 MeV alpha particles by Coulomb collisions.

It was revealed in Kolesnichenko *et al.* (2018) that the cyclotron resonance in the tokamak magnetic field can provide simultaneous interaction of high-frequency FMMs (having frequencies above the ion gyrofrequency) with MeV alpha particles at the plasma periphery and near-axis thermal ions. Due to this, inward SC of alpha particle energy can occur. The analysis carried out in Kolesnichenko *et al.* (2018) has shown that reasonable mode amplitudes are sufficient for efficient energy transfer during SC.

On the other hand, estimates show that the momentum SC can lead to a significant toroidal torque, its value weakly depending on the mode frequency (Kolesnichenko *et al.* 2020). Therefore, one could expect a considerable influence of the momentum SC on the plasma rotation in the described experiments.

In order to see whether this was the case. in the experiment we analysed the relevant JET database. Two D–T discharges (#42847 and #42856) and three deuterium discharges (#41067, #41068 and #41069) were considered. All these discharges were heated by NBI with the power $\mathcal{P}_{\rm nbi} = 10$ MW. In addition, the ICRH power was $\mathcal{P}_{\rm icrh} = 0.9$ MW and $\mathcal{P}_{\rm icrh} = 2$ MW in discharges #41067 and #41068, respectively; the alpha power was $\mathcal{P}_\alpha = 1.4$ MW and $\mathcal{P}_\alpha = 1.34$ MW in discharges #42847 and #42856, respectively. The rotation frequencies are shown in figure 1. We observe that the rotation is largest in the D–T discharge with highest performance (#42847). The exception is deuterium discharge #41067 where rotation is very large in the near-axis region. Plasma parameters in this discharge and in discharge #41068 were very similar, although ICRH power in discharge #41067 was small, $P^{\rm icrh}_{\#41067}/P^{\rm icrh}_{\#41068} \approx 1/2$. These facts demonstrate enhanced efficiency of plasma heating when the rotation is strong.

3. Change of momentum of fast ion population by destabilized modes

3.1. *Qualitative consideration of the momentum transfer from energetic ions to a destabilized mode*

We begin with a qualitative analysis of the wave–particle momentum exchange and concomitant transport processes. We will follow the approach of Kolesnichenko (1980) and Kolesnichenko *et al.* (2010*b*).

Using an analogy with quantum mechanics, we introduce plasmons (other names are quasiparticles and quantums) with the density n_k and momentum $\boldsymbol{\mathcal{M}} = \boldsymbol{k}n_k$, $\boldsymbol{k}$ is the wavevector. The plasmon density is defined by $n_k = W_k/\omega$, with W_k the wave energy density (n_k has the dimension h/V, where h is the Planck constant and V is the volume). When the waves are destabilized by fast ions with the growth rate γ_α, n_k decreases (plasmons are emitted by fast ions) with the rate $\dot{n}_k = -2\gamma_\alpha n_k$, and the momentum evolves correspondingly, $\dot{\boldsymbol{\mathcal{M}}}_\alpha = \boldsymbol{k}\dot{n}_k$, where dot over n_k denotes time derivative. This implies that the emission of plasmons generates the force acting on fast ions,

$$\boldsymbol{f}_\alpha = \dot{\boldsymbol{\mathcal{M}}}_\alpha = -2\gamma_\alpha \boldsymbol{k} n_k = -\boldsymbol{k}\frac{2\gamma_\alpha}{\omega}W_k, \tag{3.1}$$

where subscript α labels fast ions.

Note that quantum mechanics analogy is known in plasma physics, especially in nonlinear plasma theory (see, e.g. overviews Sagdeev & Galeev (1969), Fukai & Harris (1971), Tsytovich (1977) and Kadomtsev (1982)). In particular, the density of plasmons, n_k, represents the basic quantity in the theory of weak turbulence, the kinetic equation for waves is an equation for n_k, the conservation of the plasmon energy and momentum leads to conditions of the decay instability of the waves, etc.

https://doi.org/10.1017/S0022377822001039 Published online by Cambridge University Press

Equation (3.1) agrees with the known relation between the energy and momentum of a travelling wave:

$$\mathcal{M} = \frac{\text{wave energy}}{\text{phase velocity}}. \tag{3.2}$$

A question, however, arises whether (3.1) obtained by means of a simple qualitative consideration, by using quantum mechanics terminology, is applicable to realistic toroidal plasmas. The answer is given in subsequent sections, where it is shown that (3.1) correctly reflects the main features of the momentum transfer from resonant particles to the mode. Being simple, (3.1) enables one to make important conclusions immediately. Therefore, below we continue our qualitative analysis, applying (3.1) to tokamaks.

It follows from (3.1) that $\boldsymbol{f}_\alpha$ is directed along the wavevector but in the opposite direction. The wavevector is defined by $\mathrm{i}\boldsymbol{k}\tilde{X} = \nabla\tilde{X}$, where $\tilde{X}$ is a wave perturbation which we take in the form $\tilde{X} = \hat{X}(r)\exp(-\mathrm{i}\omega t + \mathrm{i}m\vartheta - \mathrm{i}n\varphi)$, with r the flux radial coordinate, ϑ and φ poloidal and toroidal angles, respectively. Then $k_\vartheta = m/r$, $k_\varphi = -n/R$, and $k_\parallel = (m\iota - n)/R = k_\varphi + \iota\epsilon k_\vartheta$, where $k_\parallel$ is the wavenumber along the magnetic field, m and n are the poloidal and toroidal mode numbers, $\iota = q^{-1}$, ι is the rotational transform, q is the tokamak safety factor, $\epsilon = r/R$, R is the major radius of the torus. The longitudinal wavenumber in many cases is small. For instance, this is the case for high frequency FMM responsible for suprathermal ICE. This is true also for low frequency modes, in particular, for Alfvén gap modes, such as TAE modes. To see it, let us take into account that the frequency of TAEs can be approximated as $\omega = |k_{\parallel *}|v_{A*}$, where the star subscript means that magnitudes are taken at r_* defined by $nq_* = m \pm 1/2$. Then

$$\left|\frac{k_\parallel}{k_\varphi}\right| = \frac{1}{2|n|q} < 1, \quad \left|\frac{k_\parallel}{k_\vartheta}\right| = \frac{\epsilon}{2|m|q} < 1, \tag{3.3a,b}$$

and k_ϑ dominates.

Because $|k_\parallel| < |k_\varphi|$, it follows from the relation $k_\parallel = k_\varphi + \epsilon\iota k_\vartheta$ that $\operatorname{sgn} k_\vartheta = -\operatorname{sgn} k_\varphi$ ($\operatorname{sgn} m = \operatorname{sgn} n$) and, hence, $\operatorname{sgn} f_\vartheta = -\operatorname{sgn} f_\varphi$. Moreover, when $|m|q \gg 1$ and/or $|n|q \gg 1$, $k_\varphi \approx -\epsilon\iota k_\vartheta$, and

$$f_\varphi \approx -\epsilon\iota f_\vartheta, \quad |f_\parallel| \ll |f_\varphi|. \tag{3.4a,b}$$

Correspondingly, the toroidal torque, $\mathcal{T}_\varphi = Rf_\varphi$, and poloidal torque, $\mathcal{T}_\vartheta = rf_\vartheta$, are connected in this case by relation

$$\mathcal{T}_\varphi \approx -\iota\mathcal{T}_\vartheta. \tag{3.5}$$

Due to relation $\epsilon\iota = B_\vartheta/B_\varphi$ (B_ϑ and B_φ are components of the equilibrium magnetic field, $\boldsymbol{B}$), (3.4*a*,*b*) implies that the product $\boldsymbol{B}\cdot\boldsymbol{f}_\alpha$ is relatively small. Nevertheless, it plays an important role because the power density lost by fast ions (P_α) is determined by $f_\parallel$:

$$P_\alpha = -f_\parallel v_{\text{res}}, \tag{3.6}$$

where $v_{\text{res}} = \omega/k_\parallel$ is the longitudinal velocity of resonant particles. This equation together with longitudinal component of (3.1) yields the expected result, $P_\alpha = 2\gamma_\alpha W_k$.

The binormal force leads to the flux of fast ions, Γ_α, across the magnetic field,

$$\Gamma_\alpha = \frac{c}{e_\alpha B^2}(\boldsymbol{f}\times\boldsymbol{B})_r = \frac{c}{e_\alpha B}(f_\vartheta b_\varphi - f_\varphi b_\vartheta) = \frac{c}{e_\alpha B}f_b, \tag{3.7}$$

where $\boldsymbol{b} = \boldsymbol{B}/B$, the subscript '$b$' labels the binormal component of a vector. This flux generates the radial electric field and the concomitant plasma rotation, both toroidal and

https://doi.org/10.1017/S0022377822001039 Published online by Cambridge University Press

poloidal. In addition, the binormal force directly affects the toroidal plasma rotation. Its toroidal component approximately equals to f_φ [$\boldsymbol{k}_b = (k_\varphi - k_\parallel b_\varphi)\boldsymbol{e}_\varphi + (k_\vartheta - k_\parallel b_\vartheta)\boldsymbol{e}_\vartheta$]. Therefore, it well exceeds toroidal component of the longitudinal force when $k_\parallel$ is small.

A more rigorous analysis below, while confirming the conclusions drawn, shows that the obtained relations are not exact. The reason is that the force $\boldsymbol{f}$ is applied to resonant particles, whereas (3.1) does not take into account specific resonances in toroidal plasmas. It will be shown that the number m should be corrected by the resonance numbers (in stellarators both m and n should be corrected for resonances associated with the lack of axial symmetry of the magnetic configurations, see e.g. Kolesnichenko *et al.* (2011)). This is not the only reason why a more rigorous analysis should be done: it is not clear what is the phase velocity in (3.1) when the mode consists of several Fourier harmonics. In addition, (3.1) cannot describe effects of finite mode width.

3.2. *Basic equations*

Let us proceed to a more rigorous description of the influence of destabilized modes on a fast ion population.

We employ a quasilinear equation for the distribution function of these ions (F) in a tokamak magnetic field,

$$\frac{\partial F}{\partial t} = \mathcal{Q}(F), \tag{3.8}$$

where $\mathcal{Q}(F)$ is a transit-time-averaged quasilinear (QL) operator determined by (39), (43), (55) and (56) of Belikov & Kolesnichenko (1982).

We restrict our analysis to shear Alfvén waves with $\omega \ll \omega_B$ (ω_B the ion gyrofrequency) and passing particles with standard orbits, $\Delta r \ll r$ (Δr is the orbit width). The variables the particle energy ($\mathcal{E} = M_\alpha v^2/2$), the magnetic moment ($\mu = \mathcal{E}_\perp/B$) and the coordinate of the particle guiding centre (r) will be used. The perturbed quantities will be labelled with a tilde and taken in the form $\tilde{X} = \mathrm{Re}\sum_m X_m(r)\exp(\mathrm{i}\psi)$, where $\psi = -\mathrm{i}\omega t + \mathrm{i}m\vartheta - \mathrm{i}n\varphi$. Using the ideal magnetohydrodynamics (MHD) approximation, we assume the longitudinal component of the perturbed electric field to vanish, $\tilde{E}_\parallel = 0$. In addition, as we are interested in Alfvén waves, we take $\tilde{B}_\parallel = 0$. This enables us to take vanishing transverse vector potential of the electromagnetic field, $\tilde{\boldsymbol{A}}_\perp = 0$, and to write the following relations:

$$\tilde{\boldsymbol{E}} = -\boldsymbol{\nabla}_\perp\tilde{\Phi}, \quad \tilde{\boldsymbol{B}} = \boldsymbol{\nabla}_\perp\times\tilde{A}_\parallel\boldsymbol{b}, \tag{3.9a,b}$$

$$\tilde{A}_\parallel = \frac{c}{\mathrm{i}\omega}\boldsymbol{\nabla}_\parallel\tilde{\Phi}, \tag{3.10}$$

where $A_\parallel$ is the longitudinal component of the vector potential, and $\tilde{\Phi}$ is scalar potential. Thus, the electromagnetic field is expressed through potential $\tilde{\Phi}$.

Due to these assumptions the QL operator of Belikov & Kolesnichenko (1982) reduces to

$$\mathcal{Q}(F) = \frac{1}{\tau_b}\sum_{m,s}\hat{\Pi}\tau_b D_{m,s}\hat{\Pi}F. \tag{3.11}$$

Here

$$D_{m,s} = \frac{\pi e_\alpha^2}{2}|\mathcal{J}_{m,s}|^2\delta(\Omega_s), \tag{3.12}$$

$$\Omega_s = \omega - k_{\parallel s}v_\parallel, \tag{3.13}$$

https://doi.org/10.1017/S0022377822001039 Published online by Cambridge University Press

$$|\mathcal{J}_{m,s}|^2 = \frac{v_D^2}{4}\left|s\Phi'_m - \frac{m}{r}\Phi_m\right|^2, \tag{3.14}$$

where $v_D = (v^2 + v_\parallel^2)/(2\omega_{B\alpha}R)$ is the particle drift velocity, $\tau_b = 2\pi qR/|v_\parallel|$ is the particle transit time, $m\Delta r/r \lesssim 1$, $k_{\parallel s} = (m_s - nq)/(qR)$, $m_s = m + s$, $s = \pm 1$, $k_\parallel(m,n) = (m - nq)/(qR)$, Φ_m is a component of the scalar potential of the electromagnetic field, $\Phi' = \mathrm{d}\Phi/\mathrm{d}r$,

$$\hat{\Pi} = \frac{\partial}{\partial\mathcal{E}} + \mathcal{L}\frac{1}{r}\frac{\partial}{\partial r}, \tag{3.15}$$

$$\mathcal{L} = \left(\frac{\omega qR}{v_\parallel} + nq\right)\frac{1}{M_\alpha\omega\omega_{B\alpha}}, \tag{3.16}$$

$\mathcal{L}(v_{\mathrm{res}}) \equiv \mathcal{L}_s = m_s/(M_\alpha\omega\omega_{B\alpha})$, v_{res} is the resonance longitudinal velocity determined by equation $\Omega_s = 0$. Note that the operator $\hat{\Pi}$ given by (3.15), (3.16) differs from that in Belikov & Kolesnichenko (1982) but it reduces to the latter at the resonance $\Omega_s = 0$.

In addition to (3.8), we will need a linear growth rate of instability. For Alfvénic perturbations we can write the following local growth rate (without damping mechanisms):

$$\gamma_\alpha = \sum_s \gamma_s, \quad \gamma_s = \frac{\pi^2}{2}\frac{e_\alpha^2 v_A^2}{c^2}\int \mathrm{d}^3\, v v_D^2 \delta(\Omega_s)\hat{\Pi}F, \tag{3.17a,b}$$

where v_A is Afvén velocity. This relation directly follows from equation $\epsilon_{11} = c^2k_\parallel^2/\omega^2$, where ϵ_{11} is a component of the dielectric tensor in a Maxwellian plasma with energetic ions, provided that $k_\vartheta v_D qR \ll v_\parallel$ and the resonance $\Omega_s = 0$ is responsible for the fast-ion interaction with Alfvén waves (Kolesnichenko 1980; Belikov, Kolesnichenko & Silivra 1992). It can also be obtained from an eigenmode equation when the mode is relatively narrow, see e.g. Kolesnichenko *et al.* (2002).

Note that normally, i.e. when the spatial inhomogeneity of energetic ions with density gradient $\mathrm{d}n_\alpha/\mathrm{d}r < 0$ drives instability, $m_s < 0$ and $n < 0$.

3.3. *'Quasilinear hydrodynamics' of particles destabilizing the mode*

Below we consider the influence of Alfvén modes on the fast-ion flux across the magnetic field, the rate of change of the fast-ion momentum and energy.

The flux surface averaged volume element in the velocity space in the tokamak magnetic field ($B = \bar{B}/h$, $h = 1 + \epsilon\cos\vartheta$) is $\mathrm{d}^3\bar{v} = \sum_\sigma \mathrm{d}\mathcal{E}\,\mathrm{d}\mu\tau_b\bar{B}/(M_\alpha^2 qR)$, where $\sigma = \mathrm{sign}\, v_\parallel$, and $\dot{\vartheta} = v_\parallel/(qR)$ was used. Taking this into account we calculate integrals $\int d^3\bar{v}GQ$ for $G = 1, M_\alpha v_\parallel, \mathcal{E}$, and $\mathcal{E}_\parallel$. After integrating by parts the term with the energy derivative we obtain

$$\int \mathrm{d}^3\,\bar{v}GQ = \sum_{m,s}\int \mathrm{d}^3\,\bar{v}\left(-\frac{\partial G}{\partial\mathcal{E}} + \frac{1}{r}\frac{\partial}{\partial r}G\mathcal{L}_s\right)D_{m,s}\hat{\Pi}F. \tag{3.18}$$

In particular, for $G = 1$ we obtain

$$\frac{\partial n_\alpha}{\partial t} = -\frac{1}{r}\frac{\partial}{\partial r}r\Gamma_\alpha, \tag{3.19}$$

where $\Gamma_\alpha = \sum_s \Gamma_{\alpha,s}$ with

$$\Gamma_{\alpha,s} = -\sum_m \frac{\pi e_\alpha^2}{8r}\mathcal{L}_s\left|s\Phi'_m - \frac{m}{r}\Phi_m\right|^2\int \mathrm{d}^3\, v v_D^2\delta(\Omega_s)\hat{\Pi}F \tag{3.20}$$

https://doi.org/10.1017/S0022377822001039 Published online by Cambridge University Press

being the particle flux across the magnetic field, which is caused by the mode.

Due to (3.17*a*,*b*), (3.20) takes the form

$$\Gamma_\alpha = -\sum_{m,s} \frac{\gamma_s k_{\vartheta,s}}{M_\alpha \omega \omega_{B\alpha}} \frac{c^2}{4\pi v_A^2} \left| s\Phi'_m - \frac{m}{r}\Phi_m \right|^2, \tag{3.21}$$

where $k_{\vartheta,s} = m_s/r$. It follows from here that the flux of resonance ions destabilizing the modes ($\gamma_\alpha > 0$) is directed outwards when the spatial gradient term dominates in (3.17*a*,*b*) and $\partial F/\partial r < 0$ (in which case $k_{\vartheta,s} < 0$). On the other hand, since the mode has finite width, $\Gamma_\alpha(r)$ is a non-monotonic function, having a maximum at a certain radius.

Using $\tilde{\boldsymbol{E}} = -\boldsymbol{\nabla}_\perp \tilde{\Phi}$, in local approximation we obtain

$$\Gamma_\alpha = -\frac{2c}{e_\alpha B} \sum_{m,s} k_{\vartheta,s} \frac{\gamma_s}{\omega} W_m, \tag{3.22}$$

where

$$W_m = \frac{c^2}{8\pi v_A^2} |\boldsymbol{E}_m|^2, \tag{3.23}$$

is the energy density of the mth harmonic of a mode (which includes both electric and magnetic perturbations, with $|\tilde{B}|^2 = (c^2/v_A^2)|\tilde{E}|^2$). Because Γ_α arises due to the $\boldsymbol{f} \times \boldsymbol{b}$ drift, as described by (3.7), (3.22) reads

$$f_b = f_\vartheta b_\varphi - f_\varphi b_\vartheta = -\sum_m k_{\vartheta,s} \frac{2\gamma_s}{\omega} W_m. \tag{3.24}$$

Now we proceed to calculations with $G = M_\alpha v_\parallel$ in (3.18). Using $\partial v_\parallel/\partial \mathcal{E} = 1/(M_\alpha v_\parallel)$ and (3.8), we obtain

$$\frac{\partial}{\partial t}\left(M_\alpha n_\alpha \langle v_\parallel \rangle\right) = \sum_{m,s} \int \mathrm{d}^3\, \bar{v} \left(-\frac{1}{v_{\mathrm{res}}} + \frac{1}{r}\frac{\partial}{\partial r} r \frac{k_{\vartheta,s} v_{\mathrm{res}}}{\omega \omega_{B\alpha}} \right) D_{m,s} \hat{I} F, \tag{3.25}$$

where $v_{\mathrm{res}} = \omega/k_{\parallel s}$, $\langle v_\parallel \rangle = \int d^3 v v_\parallel F/(M_\alpha n_\alpha)$ the average velocity of fast ions. Taking into account (3.17*a*,*b*) we can write

$$\frac{\partial}{\partial t}\left(M_\alpha n_\alpha \langle v_\parallel \rangle\right) = f_\parallel^{(1)} + f_\parallel^{(2)}, \tag{3.26}$$

where

$$f_\parallel^{(1)} = -\sum_{m,s} k_{\parallel s} \frac{2\gamma_s}{\omega} W_m, \tag{3.27}$$

$$f_\parallel^{(2)} = \sum_{m,s} \frac{\pi e^2 m_s}{8\omega_{B\alpha}\omega} \frac{1}{r}\frac{\partial}{\partial r} v_{\mathrm{res}} \left[\left| s\Phi'_m - \frac{m}{r}\Phi_m \right|^2 \int \mathrm{d}^3\, v v_D^2 \delta(\Omega_s) \hat{I} F \right]. \tag{3.28}$$

The first term in (3.26) corresponds to what is expected from analogy with quantum mechanics, as described by (3.1) with m replaced by m_s. To see the nature of the second

https://doi.org/10.1017/S0022377822001039 Published online by Cambridge University Press

term let us combine (3.28) and (3.20). This yields

$$f_{\parallel}^{(2)} = -\sum_s M_\alpha \frac{1}{r}\frac{\partial}{\partial r} r v_{\rm res} \Gamma_{\alpha,s}. \tag{3.29}$$

We observe that $f_{\parallel}^{(2)}$ is associated with the transverse particle flux generated due to the interaction of fast ions and the mode. It describes the radial redistribution of the momentum of resonant particles by the destabilized mode, not the momentum exchange between the mode and particles: $\int_0^a {\rm d}r\, r f_{\parallel}^{(2)} = 0$. Due to (3.19), (3.29) can be written in the form

$$f_{\parallel}^{(2)} = \sum_s M_\alpha v_{\rm res} \frac{\partial n_{\alpha s}}{\partial t} = \sum_s M_\alpha v_{\rm res} \int {\rm d}^3\, v Q(F). \tag{3.30}$$

Because $\int {\rm d}^3\, x f_{\parallel}^{(2)} = 0$, (3.30) implies that the redistribution of the momentum of resonance particles is just a consequence of quasilinear relaxation of distribution function. When the instability is driven by the spatial gradient of fast ions, the QL relaxation process decreases n_α at small radii and increases n_α at larger radii (for $n_\alpha' < 0$). It is clear that the presence of sources and sinks of energetic ions is required to provide a steady state value of $\int {\rm d}^3\, v Q(F)$, in which case $\partial n_\alpha/\partial t = 0$ but $\int {\rm d}^3\, v Q(F) \neq \partial n_\alpha/\partial t$ (the terms describing sources and sinks of fast ions should be added to (3.8) to make $\partial n_\alpha/\partial t = 0$ in the steady state).

Thus, the modes can transport the local momentum of fast ions even in the absence of mismatch of the regions where damping and drive dominate. We refer to this effect as mode induced redistribution (MIR). The MIR is associated with $f_{\parallel}^{(2)}$, whereas the SC is due to f_b and $f_{\parallel}^{(1)}$. Below we will see the role of poloidal and toroidal components of the forces.

Knowing $f_\parallel$ we can write

$$f_\vartheta b_\vartheta + f_\varphi b_\varphi = -\sum_{m,s} k_{\parallel s} \frac{2\gamma_s}{\omega} W_m + f_{\parallel}^{(2)}. \tag{3.31}$$

This equation should be combined with (3.24), which does not include effects of MIR and, therefore, contains components of $\boldsymbol{f}^{(1)}$. We find

$$f_\vartheta = f_\vartheta^{(1)} + f_{\parallel}^{(2)} b_\vartheta, \quad f_\vartheta^{(1)} = -\sum_{m,s} k_{\vartheta,s} \frac{2\gamma_s}{\omega} W_m, \tag{3.32a,b}$$

$$f_\varphi = f_\varphi^{(1)} + f_{\parallel}^{(2)} b_\varphi, \quad f_\varphi^{(1)} = -\sum_{m,s} k_\varphi \frac{2\gamma_s}{\omega} W_m, \quad f_b^{(2)} = 0, \tag{3.33a–c}$$

where terms of the order $b_\vartheta^2/b_\varphi^2$ are neglected.

Equations (3.24), (3.26), (3.32a,b) and (3.33a–c) prove that relation (3.1) is in agreement with the QL theory (the toroidal components of (3.1) coincides with $f_\varphi^{(1)}$, but m should be replaced with m_s in the binormal, poloidal and longitudinal components of (3.1)). On the other hand, the $\boldsymbol{f}^{(1)}$ coincides also with the force obtained within Hamiltonian approach, see Appendix A. It is clear, however, that the MIR force, $\boldsymbol{f}^{(2)}$, cannot be described by the single-particle approaches of § 3.1 and Appendix A.

In order to see the relative roles of the mode-momentum exchange and the momentum redistribution we have to estimate the ratio $f_{\parallel}^{(2)}/f_{\parallel}^{(1)}$. Assuming that the mode width is

https://doi.org/10.1017/S0022377822001039 Published online by Cambridge University Press

much less than characteristic lengths of inhomogeneity of the plasma and fast ions (L and L_α) we obtain

$$f_\parallel^{(2)} \sim \sum_{m,s} \frac{2\gamma_s k_{\vartheta,s} W_m}{\omega_{B\alpha} k_{\parallel s} \Delta_w}, \tag{3.34}$$

where $\Delta_w = (\mathrm{d}\ln W/\mathrm{d}r)^{-1}$ is a characteristic width of the mode. On the other hand, the drift term in $\hat{\Pi} F$, with $\hat{\Pi}$ given by (3.15), exceeds the term $\partial F/\partial\mathcal{E}$ with $F \propto \mathcal{E}^{-3/2}$ (which is stabilizing, $\partial F/\partial\mathcal{E} < 0$) when

$$\zeta \equiv \frac{k_{\vartheta,s} v_{\mathrm{res}}}{3 k_{\parallel s} \omega_{B\alpha} L_\alpha} > 1, \tag{3.35}$$

where $(L_\alpha)^{-1} = \mathrm{d}\ln n_\alpha/\mathrm{d}r$. It follows from (3.34), (3.35) that the ratio $f_\parallel^{(2)}/f_\parallel^{(1)}$ well exceeds unity, being a product of ζ and a large multiplier,

$$\frac{f_\parallel^{(2)}}{f_\parallel^{(1)}} \sim \zeta \frac{3L_\alpha}{\Delta_w} \gg 1. \tag{3.36}$$

Equations (3.8) and (3.18) with $G = \mathcal{E}$ reduce to

$$\frac{\partial}{\partial t}\left(M_\alpha n_\alpha \langle\mathcal{E}\rangle\right) = P^{(1)} + P^{(2)}, \tag{3.37}$$

where $P^{(1)}$ represents the fast-ion power sink because of the instability,

$$P^{(1)} = -\sum_m 2\gamma_\alpha W_m, \tag{3.38}$$

and $P^{(2)}$ is the redistributed power

$$P^{(2)} = \frac{1}{r}\frac{\partial}{\partial r} \sum_{m,s} \int \mathrm{d}^3 v \mathcal{E} D_{m,s} \hat{\Pi} F. \tag{3.39}$$

When $G = \mathcal{E}_\parallel$, we obtain

$$P_\parallel^{(1)} = P^{(1)} = \sum_s f_{\parallel,s}^{(1)} v_{\mathrm{res}}, \tag{3.40}$$

which is a consequence of the fact that the resonance mode–particle interaction does not affect particle transverse velocities distribution, and

$$P_\parallel^{(2)} = \sum_s \frac{M_\alpha v_{\mathrm{res}}^2}{2} \frac{\partial n_{\alpha s}}{\partial t}, \tag{3.41}$$

which is similar to (3.30).

https://doi.org/10.1017/S0022377822001039 Published online by Cambridge University Press

3.4. *Momentum transfer to gap modes*

3.4.1. *Simple gap mode*

We restrict first our analysis to a gap mode consisting of two harmonics with the poloidal mode numbers m and $m+\mu$ but with the same n, where $\mu = \pm 1$ for TAE modes, $\mu = \pm 2$ for EAE modes, etc.

We begin with a consideration of the forces arising due to resonance mode–particle interaction at the r_* radius defined by $k_{\|1}(r_*) + k_{\|2}(r_*) = 0$, where $nq_* = m + \mu/2$ and $k_{\|1}(r_*)q_*R = -k_{\|2}(r_*)q_*R = -\mu/2$. The subscripts 1 and 2 label magnitudes relevant to the m and $m+\mu$ harmonics, respectively. The resonance numbers ($s = \pm 1$) should satisfy equation

$$s_1 + s_2 = 0, \tag{3.42}$$

in order to provide $k_{\|1,s_1}(r_*) + k_{\|2,s_2}(r_*) = 0$. Then we obtain from (3.27) that $f_{\|*}^{(1)} = 0$, provided that the difference between $W_{m_1}(r_*)$ and $W_{m_2}(r_*)$ is negligible. On the other hand, because $m + \mu/2 = nq_*$, the condition $k_{\|1}(r_*) + k_{\|2}(r_*) = 0$ leads to $k_{\bar{m},*} = 0$, where $k_{\bar{m},*} = (\bar{m}\iota_* - n)/R$ is the longitudinal wavenumber with $\bar{m} = 0.5(m_1 + m_2) = 0.5(m_{s_1} + m_{s_2})$ at $r = r_*$. Taking $k_\|$ with the poloidal mode number $\bar{m}$ we obtain from (3.1) the longitudinal force $f_{\|*} = 0$. The poloidal component of (3.1) with $\bar{m}$ is

$$f_{\vartheta *} = -\frac{\bar{m}}{r_*}\frac{2\gamma_\alpha}{\omega}W. \tag{3.43}$$

This corresponds to (3.32*a*,*b*) for $f_{\vartheta *}^{(1)}$. Thus, (3.1) with $k_\vartheta = \bar{m}/r$ correctly describes the rate of momentum exchange between the gap modes and fast ions.

The presence of the magnetic shear can strongly break the antisymmetry of the wavenumbers $k_{\|1,s_1}$ and $k_{\|2,s_2}$ at $r \neq r_*$, making $k_{\|s}$ of a gap mode not vanishing and considerable. To see this we approximate the mode frequency by $\omega = |k_{\|*}|v_{A*}$. Then the resonance condition ($\omega = k_{\|s}v_{\rm res}$) for these harmonics at the radius $r = r_* + \Delta r$, where $\iota = \iota_* + \Delta\iota$, can be written as follows:

$$\left[\operatorname{sgn} k_{\|1*} + \frac{2s_1}{\mu} + \frac{2(m+s_1)}{\mu}\frac{\Delta\iota}{\iota_*}\right] v_{\rm res}^{(m)} = v_{A*}, \tag{3.44}$$

$$\left[\operatorname{sgn} k_{\|2*} + \frac{2s_2}{\mu} + \frac{2(m+\mu+s_2)}{\mu}\frac{\Delta\iota}{\iota_*}\right] v_{\rm res}^{(m+\mu)} = v_{A*}, \tag{3.45}$$

where $\operatorname{sgn} k_{\|1*} = -\operatorname{sgn} k_{\|2*} = -1$, s_1 and s_2 satisfy (3.42). We observe that while $v_{\rm res}^{(m)}$ and $v_{\rm res}^{(m+\mu)}$ have different signs at r_*, the signs of the terms proportional to $\Delta\iota$ are the same for both harmonics. This implies that $|v_{\rm res}|$ of one of the harmonics grows, whereas $|v_{\rm res}|$ of another one decreases as r moves away from r_*. For instance, taking $s_1 = 1$ we obtain for TAE modes,

$$v_{\rm res}^{(m)} = \frac{v_{A*}}{1 + 2(m+1)\Delta\iota/\iota_*}, \tag{3.46}$$

$$v_{\rm res}^{(m+1)} = -\frac{v_{A*}}{1 - 2m\Delta\iota/\iota_*}. \tag{3.47}$$

In particular, at the radius r_m where $q = m/n$ (3.46), (3.47) yield

$$v_{\rm res}^{(m)} = \frac{v_{A*}}{1 + (m+1)/m}, \tag{3.48}$$

$$v_{\rm res}^{(m+1)} = -\infty. \tag{3.49}$$

https://doi.org/10.1017/S0022377822001039 Published online by Cambridge University Press

Here we took into account that $(\iota_m - \iota_*)/\iota_* = 1/(2m)$, with $\iota_m = \iota(r_m)$.

Because of this, $|v_{\rm res}|$ can exceed the maximum velocity of the energetic ions, v_α, at certain radii within the mode width, leading to $k_\parallel$ determined by another harmonic only, which decreases the growth rate but may increase of $f_\parallel$. In contrast, when $|v_{\rm res*}| < v_A$, the increase of the resonance velocity can destabilize the mode. Presumably, this was the case in the Large Helical Device stellarator where odd and even TAEs were observed (Kolesnichenko *et al.* 2004).

Below we exclude from the consideration these particular cases to see effects of the shear only and employ (3.27) with two harmonics equally contributing to γ_s and with $W_m = W_{m+\mu}$. Then the summation in (3.27) over m reduces to calculation of

$$k_{\parallel s}^{\Sigma} \equiv \sum k_{\parallel s} = \omega \left(\frac{1}{v_{\rm res}^{(m)}} + \frac{1}{v_{\rm res}^{(m+\mu)}} \right). \tag{3.50}$$

Combining (3.44) and (3.45) we obtain

$$\frac{k_{\parallel s}^{\Sigma}(\iota)}{|k_{\parallel 1*}|} = \frac{4nq_*}{\mu} \frac{\Delta\iota}{\iota_*} \tag{3.51}$$

and

$$k_{\parallel s}^{\Sigma} = \frac{2n}{R} \frac{\Delta\iota}{\iota_*}, \quad \frac{k_{\parallel s}^{\Sigma}}{k_\varphi^{\Sigma}} = -\frac{\Delta\iota}{\iota_*}, \tag{3.52a,b}$$

where $k_\varphi^{\Sigma} = 2k_{\varphi 1}$, $|\Delta\iota|/\iota_* \lesssim 1/(2|m|)$. The force $f^{(1)}$ is maximum at the radius where the product $k_{\parallel s}^{\Sigma}\gamma_s W$ is largest.

Note that for narrow modes the ratio $\Delta\iota/\iota_*$ can be approximated by $\Delta\iota/\iota_* = -\hat{s}\Delta r/r_*$, where $\hat{s}$ is the magnetic shear.

3.4.2. *Multiple-harmonic gap mode*

Now we proceed to analysis for modes consisting of more than two harmonics, such as global TAE. Because the mode amplitudes of the pairs of coupled harmonics are localized around certain radii, each pair can be treated independently. In TAEs harmonics with m and $m+1$ are coupled in the region between the $q_m = m/n$ and $q_{m+1} = (m+1)/n$ rational flux surfaces; the width of this region is $\Delta q = 1/n$. Therefore, when the mode occupies a certain region $(\Delta q)_{mode}$, the number of coupled harmonics can be $n(\Delta q)_{mode} + 1$. Using (3.52a,b), we can evaluate the longitudinal force $f^{(1)}$ produced by one pair of harmonics by (3.27) with $k_{\parallel s} \sim 1/(qR)$, the total force produced by the mode with $n \gg 1$ has $k_\parallel^{\rm mode} \sim n/(qR)$, with some average q. This overestimates $k_\parallel^{\rm mode}$ and, hence, $f_{\rm mode}^{(1)}$, when only a few harmonics have large local growth rate.

The wavenumber $k_{\parallel s}$ is not the only factor that determines $f^{(1)}$: it is of importance where maxima of $|\mathcal{J}_{m,s}|^2$ are located.

4. Plasma rotation and generation of the electric field

To study the rotation caused by destabilized eigenmodes we proceed from the equation obtained by summing equations of motion for the electrons, bulk plasma ions and energetic ions. As in the works of Kolesnichenko *et al.* (2010a,b), we neglect several terms. First, the electron and fast-ion inertial terms, whose contribution is much less than that of the bulk plasma ions. Second, the pressure-gradient terms, which implies that we are considering effects superposed on the neoclassical transport. Third, the centrifugal term which is beyond applicability of our equations, being proportional to $\tilde{E}^4$.

https://doi.org/10.1017/S0022377822001039 Published online by Cambridge University Press

We consider first the binormal component of this equation which contains the binormal force acting on fast ions due to their emission of the momentum: as shown in § 3, the binormal force leads to the transverse fast ions flux across, i.e. produces the radial electric current, $j_{\alpha r}$, which generates the radial electric field, E_r, and can affect plasma rotation. In the cylindrical approximation we can write

$$M_i n_i \dot{u}_{ib} = \sum_{\sigma=e,i,\alpha} f^{(1)}_{\sigma b} + f^{\rm vis}_{ib} - \frac{1}{c}\overline{Bj_r}. \tag{4.1}$$

The following notations are used: $\boldsymbol{u}_i = \bar{\boldsymbol{V}}_i$ is the bulk plasma ion hydrodynamic velocity ($\boldsymbol{V}_i$) averaged over flux surface, a bar over letters denotes flux surface averaging (below can be omitted), $\boldsymbol{f}^{(1)}_{\sigma}$ is the force acting on the σ species due to emission/absorption of the momentum, $\boldsymbol{f}^{\rm vis}_i$ is associated with the ion viscosity or other mechanisms braking the rotation (discussed at the end of this section), a dot over letters denotes a time derivative, $\boldsymbol{j}$ is the overall current density ($\boldsymbol{j} = \sum_{\sigma=\alpha,e,i}\boldsymbol{j}_\sigma$) induced by destabilized modes.

The radial current on the right-hand side of this equation can be expressed through a time derivative of the radial electric field, as follows from the curl-free Maxwell equation,

$$\dot{E}_r + 4\pi j_r = 0. \tag{4.2}$$

On the other hand,

$$\dot{u}_{ib} = -c\dot{E}_r/B \tag{4.3}$$

on the left-hand side, which is obtained from the radial component of the equation of motion for the ion component in the assumption of small $\dot{u}_{ir}$ and $\partial(\nabla_r p_i)\partial t$. Due to these last two relations, (4.1) takes the form

$$\dot{E}_r = -\frac{B}{cM_i n_i}\left(\sum_{\sigma=e,i,\alpha} f^{(1)}_{\sigma b} + f^{\rm vis}_{ib}\right) - \frac{v_A^2}{c^2}\dot{E}_r. \tag{4.4}$$

We observe that the last term on the right-hand side is much less than the left-hand side term. The reason is that the bulk plasma current arising in response to the fast ion current almost compensates the latter.

The physics of this phenomenon is the following: the resonant interaction of the mode and fast ions leads to the radial flux described by, for example, (3.7) which generates the radial electric field and concomitant radial current of the bulk plasma particles. We found that this current is almost equal to the fast-ion current. In other words, the overall current density, $j_r = \sum_{\sigma=e,i,\alpha} j_{\sigma r}$, is small, the term Bj_r/c in (4.1) is less than the inertia term on the left-hand side of this equation by a factor of v_A^2/c^2.

Therefore, below we neglect the last term in (4.4).

Note that in the absence of SC, i.e. when the region driving the instability coincides with the damping region, $\sum_\sigma f^{(1)}_{\sigma b} = 0$ (the diffusion of resonance particles is intrinsically ambipolar, see e.g. Kolesnichenko *et al.* (2010*b*)) and (4.4) yields $E_r = 0$.

The cylindrical approximation adopted in (4.1) underestimates the role of inertia. Coupling of the poloidal motion to the toroidal one in axisymmetric toroidal configurations enlarges the plasma inertia in the poloidal rotation by a factor $\mathcal{K} \approx 1 + 2q^2$, see Helander & Sigmar (2005) and Appendix B. Therefore, equations that determine

https://doi.org/10.1017/S0022377822001039 Published online by Cambridge University Press

poloidal and toroidal velocities are (the terms proportional to j_r are neglected)

$$\mathcal{K}M_i n_i \dot{u}_{i\vartheta} = \sum_{\sigma=e,i,\alpha} f^w_{\sigma\vartheta} + f^{\rm vis}_{i\vartheta}, \tag{4.5}$$

$$M_i n_i \dot{u}_{i\varphi} = \sum_{\sigma=e,i,\alpha} f^w_{\sigma\varphi} + f^{\rm vis}_{i\varphi}, \tag{4.6}$$

where $\boldsymbol{f}^w = \boldsymbol{f}^{(1)} + \boldsymbol{f}^{(2)}$.

The electric field is determined by (4.2) which can be written as

$$c\dot{E}_r + \dot{u}_{i\vartheta}\bar{B}_\varphi - \dot{u}_{i\varphi}\bar{B}_\vartheta = 0. \tag{4.7}$$

Assuming that $E_r = 0$ before the instability (we consider effects superposed on the neoclassical magnitudes) we can remove dots over letters.

The $\boldsymbol{E}\times\boldsymbol{B}$ drift leads to velocities u^E_ϑ and u^E_φ determined by

$$u^E_\vartheta = -c\frac{E_r B_\varphi}{B^2}, \tag{4.8}$$

$$u^E_\varphi = c\frac{E_r B_\vartheta}{B^2}, \tag{4.9}$$

so that the poloidal flow dominates. However, toroidicity and trapped particles decrease the poloidal velocity, whereas the toroidal force, f_φ, can increase the toroidal velocity. Below we consider this issue.

It follows from (4.7) that the radial electric field is associated with both poloidal rotation and toroidal rotation. The poloidal and toroidal motions are decoupled only in the limit cases $\mathcal{S} \gg 1$ and $\mathcal{S} \ll 1$, where

$$\mathcal{S} = \frac{u_\varphi B_\vartheta}{u_\vartheta B_\varphi} = \frac{\Omega_\varphi}{q\Omega_\vartheta}, \tag{4.10}$$

and $\Omega_\vartheta = v_\vartheta/r$, $\Omega_\varphi = v_\varphi/R$ the rotation frequencies. Note that non-averaged motion can be completely decoupled only in the toroidal direction, see Appendix B and Helander & Sigmar (2005). When $\mathcal{S} \ll 1$, (4.7) determines the poloidal flow which coincides with the $\boldsymbol{E}\times\boldsymbol{B}$ flow,

$$u_\vartheta = -c\frac{E_r}{B} \approx u^E_\vartheta. \tag{4.11}$$

However, $u_\varphi \gg u^E_\varphi$ when $\mathcal{S} \gg 1$:

$$u_\varphi = c\frac{E_r}{B_\vartheta} = \frac{u^E_\varphi}{\Theta^2}, \tag{4.12}$$

where $\Theta = B_\vartheta/B_\varphi \ll 1$.

For $\mathcal{S} \sim 1$, although the poloidal and toroidal motion equally contribute to (4.7), toroidal velocity dominates, $u_\varphi/u_\vartheta \sim \Theta^{-1} \gg 1$, and the ratio of angular velocities is $\Omega_\varphi/\Omega_\vartheta \sim q$.

Note that in neoclassical theory $u^{\rm neo}_\vartheta/v_{i,\rm th} \sim \rho_i/L$ ($v_{i,\rm th}$ the ion thermal velocity, ρ_i the ion Larmor radius, L a characteristic inhomogeneity length), therefore normally $\mathcal{S} \gg 1$ but

$$u^{\rm neo}_\varphi = \frac{c}{B_\vartheta}\left(E_r - \frac{1}{n_\sigma e_\sigma}\frac{{\rm d}p_\sigma}{{\rm d}r}\right). \tag{4.13}$$

Thus, we have to evaluate $\mathcal{S}$, which requires estimates for u_φ and u_ϑ.

https://doi.org/10.1017/S0022377822001039 Published online by Cambridge University Press

In the unstable region we can write

$$u_{i\vartheta} = \frac{1}{M_i n_i \mathcal{K}} f^w_{\alpha\vartheta} (\Delta t)_\vartheta, \tag{4.14}$$

$$u_{i\varphi} = \frac{1}{M_i n_i} f^w_{\alpha\varphi} (\Delta t)_\varphi, \tag{4.15}$$

where $(\Delta t)_\varphi \leqslant \tau_\varphi^{\rm vis}$ and $(\Delta t)_\vartheta \leqslant \tau_\vartheta^{\rm vis}$ are characteristic times. At the initial stage of instability, i.e. when the viscosity and other braking mechanisms are negligible, $(\Delta t)_\varphi = (\Delta t)_\vartheta$. Then for $f = f^{(1)}$ we obtain $\mathcal{S} \equiv \mathcal{S}_0$ and $(\Omega_\varphi/\Omega_\vartheta)_0$ with

$$\mathcal{S}_0 = \mathcal{K}\Theta \frac{f^{(1)}_{\alpha\varphi}}{f^{(1)}_{\alpha\vartheta}} = (1 + 2q^2)\Theta^2 \frac{nq}{m}, \quad \left(\frac{\Omega_\varphi}{\Omega_\vartheta}\right)_0 = q\mathcal{S}_0. \tag{4.16a,b}$$

We conclude that $\mathcal{S}_0 \sim \epsilon^2$ and $(\Omega_\varphi/\Omega_\vartheta)_0 \sim q\epsilon^2$ for $m \sim nq$. In this case the poloidal velocity represents the $\boldsymbol{E} \times \boldsymbol{B}$ drift and the poloidal frequency dominates when $q\epsilon^2 \ll 1$. In the presence of the MIR force, such that $f^{(2)}_\varphi \sim f^{(1)}_\vartheta$, $\mathcal{S}_0 \sim \mathcal{K}\Theta \sim 1$ for $q \sim 1.5$ and $\epsilon \sim 0.2$.

In the later stage of instability, rotation braking becomes important. The braking mechanisms have been extensively studied (see, e.g. the overview Ida & Rice (2014)). The poloidal rotation braking may be determined by neoclassical or anomalous processes. In both cases, the damping occurs via friction between trapped and passing ions. As a result, the poloidal velocity evolution after a change in the driving force is non-exponential because of the complicated rearrangement of the pitch-angle distribution (Morris, Haines & Hastie 1996). However, it seems to be reasonably approximated by an exponent with a characteristic time $\sim \tau_{ii}$ (Morris *et al.* 1996; Hinton & Rosenbluth 1999). For the toroidal rotation in axisymmetric configurations, the braking via friction between trapped and passing particles is impossible, whereas the neoclassical viscous braking is weak. Therefore, the toroidal braking results from turbulence and/or symmetry breaking of the magnetic field (ripple, resonant magnetic perturbations, etc.). The turbulent momentum transport is characterized by the Prandtl number (the ratio of ion thermal diffusivity to the perpendicular viscosity coefficient). In experiments, it was found to be less than unity in JET (Weisen *et al.* 2012) and larger than unity in TFTR (Scott *et al.* 1990) (experiments on other devices are mentioned in Ida & Rice (2014)), but it seems to be ~ 1. The toroidal flow damping due to field ripple was observed in experiments with artificially enhanced ripple (e.g. in JET de Vries *et al.* (2010), see also another in Ida & Rice (2014)). The magnetic braking due to resonant magnetic perturbations may be strong but we will not consider this case here.

We conclude that in the steady state we can use (4.14) and (4.15) with $(\Delta t)_\vartheta \sim \tau_{ii}$ and $(\Delta t)_\varphi \sim \tau_E (\Delta r)^2/a^2$, where τ_E is the overall energy confinement time, and Δr is a characteristic radial extent of the region where the momentum transport takes place. Then the toroidal velocity exceeds the poloidal one when

$$\frac{f^w_{\alpha\varphi}}{f^w_{\alpha\vartheta}} \frac{\tau_E}{\tau_{ii}} \left(\frac{\Delta r}{a}\right)^2 > 1, \tag{4.17}$$

in which case the contribution of the $E \times B$ drift to toroidal velocity is negligible. It is clear that the estimate (4.17) is true when the unstable mode exists for $(\Delta t)_{\rm mode} > \max[(\Delta t)_\vartheta, (\Delta t)_\phi]$.

https://doi.org/10.1017/S0022377822001039 Published online by Cambridge University Press

5. Application to ITER

In order to see whether effects of the SC and MIR can be considerable, we have to make numerical estimates. We selected a global TAE in the ITER 15 MA baseline scenario, which is located in the region $0.6 \leqslant r/a \leqslant 0.8$ and has $n = 20$ (Pinches *et al.* 2015). This mode is destabilized by alpha particles and NBI deuterons with the local growth rate $\gamma_\alpha/\omega \sim 10^{-2}$. Relevant parameters are: $R = 6.2$ m; $a = 2$ m; $B = 5.3$ T; plasma elongation $\kappa = 1.7$; plasma volume $V_p = 830$ m^3; NBI power $\mathcal{P}_{\rm nbi} = 33$ MW; $v_\alpha = 1.3 \times 10^7$ m s^{-1}; $v^D_{\rm beam} = 10^7$ m s^{-1}; $v_A = 7 \times 10^6$ m s^{-1}; $q \sim 1.5$ at $r/a \sim 0.7$ (Pinches *et al.* 2015). The mode amplitudes are not known. We take $\tilde{B}/B = 10^{-4}$, which is realistic.

We infer from this the following. The poloidal mode numbers vary from $m \sim 20$ to $m \sim 30$. The toroidal force $f^{(1)}_{\alpha,\varphi}$ is

$$f^{(1)}_{\alpha,\varphi} = 2\frac{n}{R}\frac{\gamma_\alpha}{\omega}\left(\frac{\tilde{B}}{B}\right)^2 \frac{B^2}{8\pi} = 7.2 \times 10^{-3}\frac{\rm N}{\rm m^3}. \tag{5.1}$$

Its ratio to the volume averaged NBI force, $\langle f^{\rm NBI}_\varphi\rangle = \chi_{\rm beam}\mathcal{P}_{\rm nbi}/(V_p v_{\rm beam})$ with $\chi_{\rm beam} = v_\varphi/v_{\rm beam}$, is

$$\frac{f^{(1)}_{\alpha,\varphi}}{\langle f^{\rm NBI}_\varphi\rangle} = \frac{n}{4\pi}\frac{\gamma_\alpha}{\omega}\frac{\tilde{B}^2 V_p v_{\rm beam}}{\chi_{\rm beam}\mathcal{P}_{\rm nbi}R} = 3.6. \tag{5.2}$$

It follows from here that the toroidal torque produced by SC can exceed that of NBI, especially at the plasma periphery, $r/a \sim 0.7$, where $f^{\rm NBI}_\varphi < \langle f^{\rm NBI}_\varphi\rangle$. Note that other mode-induced forces, except for $f^{(1)}_\parallel$, are even larger than $f^{\rm NBI}_\varphi$:

$$\frac{f^{(1)}_\vartheta}{f^{(1)}_\varphi} = \frac{m_s}{\epsilon n} \sim 5, \quad \frac{f^{(1)}_\parallel}{f^{(1)}_\varphi} = \frac{1}{2\epsilon nq} = \frac{1}{60}, \quad \frac{f^{(2)}_\parallel}{f^{(1)}_\varphi} \sim 4. \tag{5.3a–c}$$

Knowing forces and assuming that $(\Delta t)_\varphi$ and $(\Delta t)_\vartheta$ are less than the mode duration, we can write the following estimates for the generated electric field and plasma rotation in the steady state due to SC:

$$|E_r| \sim \frac{B}{cM_i n_i \mathcal{K}}|f^{(1)}_\vartheta|(\Delta t)_\vartheta, \quad |u_\varphi| \sim \frac{1}{M_i n_i}|f^{(1)}_\varphi|(\Delta t)_\varphi, \tag{5.4a,b}$$

where $(\Delta t)_\vartheta = \tau_{ii}$ and $(\Delta t)_\varphi = \tau_E(\Delta r)^2/a^2$ with Δr a characteristic distance between the regions of drive and damping. We take $\tau_E = 3$ s (Green *et al.* 2003), $\Delta r = 0.5(\Delta r)_{\rm mode} = 0.1a$. Then in the region of mode location $(\Delta t)_\vartheta \sim 0.01$ s and $(\Delta t)_\varphi \sim 0.03$ s, which leads to $E_r \sim 1$ kV m^{-1} and $u_\varphi = 500$m s^{-1}.

For comparison, we calculate the toroidal velocity in JET. According to figure 1, $\Omega_\varphi = (1\text{–}2) \times 10^4$ rad s^{-1} at $R \sim 3.4$ m. Then the flux surface averaged toroidal velocity can be evaluated as $u_\varphi = (3\text{–}6) \times 10^4$ m s^{-1}. This well exceeds the calculated velocity in ITER. However, in reality the mode amplitude may exceed $\tilde{B}/B = 10^{-4}$. For instance, for $\tilde{B}/B = 10^{-3}$, we obtain that the rotation velocity in ITER approximately that in JET and $E_r \sim 100$ kVm^{-1}.

We remind that the generated electric field and the rotation velocity as well have opposite directions in the driving region and the damping region during SC. This means that they produce sheared rotation within the mode width.

https://doi.org/10.1017/S0022377822001039 Published online by Cambridge University Press

6. Summary

The results of this work can be summarized as follows.

The change of momentum of energetic ions because of MHD modes destabilized by these ions and the concomitant sheared plasma rotation in tokamaks are studied. Both a quasilinear theory and a Hamiltonian approach are used to consider the mode–particle momentum exchange. The plasma rotation is studied by employing a flux surface equation obtained by summing up plasma fluid equations of motion for different particle species, where the influence of toroidicity on the ion inertia term is taken into account.

In the framework of quasilinear theory, the analysis is carried out for Alfvénic modes destabilized due to spatial inhomogeneity of the energetic ions. The moments of a two-dimensional QL operator are calculated. This enabled us to formulate MHD-like equations for the particle density, momentum and power density, which contain the transverse flux of fast ions, the forces (in particular, the binormal force f_b and the longitudinal forces $f_\parallel^{(1)}$, $f_\parallel^{(2)}$) acting on fast ions, and the power absorbed and radially redistributed due to the mode. As a result, two mechanisms of the influence of destabilized modes on the momentum of resonance particles are revealed. First, emission and absorption of momentum (resulting in the forces f_b, $f_\parallel^{(1)}$), which can lead to SC of the momentum of fast ions exciting the instability. Second, redistribution of the momentum of fast ions (resulting in the force $f_\parallel^{(2)}$), which is a consequence of finite mode width – a phenomenon called MIR.

The same forces (except for the MIR force) are obtained by applying a Hamiltonian approach. It is found that these forces persist even when the wave frequency is not small compared with the ion gyrofrequency.

It is concluded that the binormal force arising due to wave emission (f_b) leads to the transverse flux of fast ions and the concomitant radial electric current, $j_r^{(\alpha)}$, during SC, i.e. when the region driving the instability does not coincide with the damping region. The current $j_r^{(\alpha)}$ is compensated to a large extent by the arising plasma current. However, the resulting current is still sufficiently large to generate a considerable radial electric field according to equation $\dot{E}_r + 4\pi j_r = 0$.

In contrast, the MIR force, $f_\parallel^{(2)}$, is not associated with the radial electric field; it can transport the local momentum of fast ions even in the absence of mismatch of the regions where damping and drive dominate.

Both f_b and $f_\parallel$ affect toroidal rotation. However, when $k_\parallel/k \ll 1$ (typically, the case of TAEs), $f_\parallel^{(1)}$ is small. For this reason, the force f_φ responsible for the toroidal rotation is mainly determined by the toroidal component of the binormal force $(\boldsymbol{f}_b)_\varphi$ and $f_\parallel^{(2)}$. It is shown that the binormal momentum is rapidly, on the time scale of approximately particle transit time, redistributed between fast ions, thermal ions and electrons, so that all the species are accelerated almost simultaneously. In contrast, the longitudinal momentum exchange between species takes place on much longer time scales.

Because $f_\vartheta^{(1)} \gg f_\varphi^{(1)}$, poloidal rotation dominates during the initial stage of instability being determined by the $\boldsymbol{E} \times \boldsymbol{B}$ drift. However, because of braking mechanisms (such as viscosity, magnetic ripple, collisions between passing and trapped ions), in the later stage it can be suppressed; then the toroidal velocity exceeds the poloidal one, and its magnitude well exceeds the $\boldsymbol{E} \times \boldsymbol{B}$ drift velocity.

Note that the mode amplitude is a free parameter in our theory. Due to this, our theory is applicable to experiments with any mode amplitudes, regardless of the mechanism which limits it. Various mechanisms are known that can determine mode amplitudes, see e.g. review papers (Gorelenkov, Pinches & Toi 2014; Chen & Zonca 2016; Todo 2019).

https://doi.org/10.1017/S0022377822001039 Published online by Cambridge University Press

Our estimates for ITER where a global TAE with $n = 20$ and $m = 20$–30 is predicted (Pinches *et al.* 2015) show that the mode-induced forces can be significant, being even larger than the toroidal force caused by NBI. This result may produce an illusion that the expected influence of the mode-induced forces on plasma rotation can be unrealistically large, and a question then arises whether the obtained relations for these forces are correct. In connection with this, we remind that the forces arising due to emission of the momentum are evaluated in three independent ways: first, by using quantum mechanics analogy; second, by quasilinear theory; and third, by Hamiltonian formalism. All these three techniques lead to the same result: first, they give exactly the same relation for the toroidal force; second the presence of m in the poloidal and other components of relation (3.1) instead of $m_s = m \pm 1$ predicted by (3.24), (3.26), (3.32*a*,*b*) and (A5), (A6) is not important for estimates because $m \gg 1$. The MIR force is found only in a quasilinear theory, but it has a clear physical meaning and thus it should be correct, too. In spite of large values of these forces, their overall effect can be moderate or even small. The matter is that the forces vary radially and can have opposite directions in the layers located very close to each other, in which case they tend to compensate each other because of viscosity. In seems, this is the situation in ITER with the MIR force produced by a multicomponent TAE. On the other hand, effects of the SC forces strongly depend on the radial location of driving and damping regions, they are weak when these regions considerably overlap. Therefore, although our estimates indicate strong forces produced by the destabilized TAE mode in ITER, a detailed information on the mode features (driving and damping mechanisms, the mode structure and amplitude, etc.) and plasma viscosity is required for a reliable prediction of sheared rotation caused by of SC and MIR in particular scenarios of ITER. This issue deserves further study.

Acknowledgements

This work has been carried out within the framework of the EUROfusion Consortium, funded by the European Union via the Euratom Research and Training Programme (grant agreement no. 101052200 – EUROfusion). Views and opinions expressed are, however, those of the author(s) only and do not necessarily reflect those of the European Union or the European Commission. Neither the European Union nor the European Commission can be held responsible for them. The work was also supported by the project no. PL27/21-N of the National Academy of Sciences of Ukraine.

Editor P. Helander thanks the referees for their advice in evaluating this article.

Declaration of interests

The authors report no conflict of interest.

Appendix A. Momentum exchange of particles with an eigenmode: Hamiltonian approach

The aim of this appendix is to demonstrate that the relationships between energy and momentum transferred from a particle to a mode, which were obtained in § 3, can be recovered from analysis of motion of separate particles.

We proceed from the particle Hamiltonian in action-angle coordinate system (Kaufman 1972),

$$H(J_\xi, J_\theta, J_\phi, \xi, \theta, \phi, t) = H_0(J_\xi, J_\theta, J_\phi) + \tilde{H}(J_\xi, J_\theta, J_\phi, \xi, \theta, \phi, t), \tag{A1}$$

where ξ, θ and ϕ are the canonical gyro-, poloidal and toroidal angles, J_θ and J_ϕ are the respective actions, $H_0 = \mathcal{E}$ and $\tilde{H}$ describe the motion in the absence of the wave and the

https://doi.org/10.1017/S0022377822001039 Published online by Cambridge University Press

wave effect, respectively. For passing particles, the canonical poloidal and toroidal angles do not differ much from the magnetic angles ($\theta \approx \vartheta$, $\phi \approx \varphi$); J_ϕ is exactly the canonical angular momentum in the ϕ-direction, and J_θ is the canonical angular momentum up to small corrections caused by toroidicity.

Expanding the wave contribution into a Fourier series, we write

$$\tilde{H} = \sum_j \tilde{H}_j \exp(-\mathrm{i}\omega t + \mathrm{i}j\theta - \mathrm{i}n\phi + \mathrm{i}l\xi), \tag{A2}$$

where we have neglected the dependence of $\tilde{H}_j$ on action variables. The spectrum of j-values for which the coefficients $\tilde{H}_j$ are significant depends on the mode and resonance type; for example, the values $j = m \pm 1$ are the largest for the mode with the poloidal number m interacting with a particle via the sideband Cherenkov resonance. We will consider the effect of a single resonance

$$\omega = j\omega_\theta - n\omega_\phi + l\omega_\xi, \tag{A3}$$

where ω_θ and ω_ϕ are the frequencies of the particle motion in the θ- and ϕ-directions, respectively; ω_ξ is the bounce-averaged cyclotron frequency. Then we can disregard all harmonics except one in (A2). One can see that

$$\frac{\dot{H}_0}{\omega} = \frac{\dot{J}_\phi}{-n} = \frac{\dot{J}_\theta}{j} = \frac{\dot{J}_\xi}{l} = -\mathrm{i}H_j \exp(-\mathrm{i}\omega t + \mathrm{i}j\theta - \mathrm{i}n\phi + \mathrm{i}l\xi). \tag{A4}$$

Hence, the forces acting on the particle and the power transferred to the wave satisfy the relationship

$$\frac{\hat{P}_\alpha}{-\omega} = \frac{\hat{f}_\varphi}{k_\varphi} = \frac{\hat{f}_\vartheta}{k_{\vartheta,j}} \tag{A5}$$

where $k_\varphi = -n/R$, $k_{\vartheta,j} = j/r$ and the 'hats' indicate that the quantities are taken for a single ion (rather than for the fluid, as in the main text of the paper). Now we can find $\hat{f}_\parallel$. To main order in ϵ, (A5) yields

$$\hat{f}_\parallel = \hat{f}_\varphi + \frac{\epsilon}{q}\hat{f}_\vartheta = -\frac{k_{\parallel,j}}{\omega}\hat{P}_\alpha \tag{A6}$$

with $k_{\parallel,j} = (j\iota - n)/R$. These relationships agree with (3.27), (3.32*a*,*b*) and (3.33*a*–*c*). Thus, the proportionality between the forces acting on the fast ions from the wave and the transferred energy, which was obtained above, first, from quantum-mechanics considerations and, second, from quasilinear theory, follows also from equations of motion of each single particle.

Now let us find $\dot{r}$ and $\dot{v}_\parallel$. Using equations

$$J_\phi = -\frac{e}{c}\psi_p + Mv_\parallel R, \tag{A7}$$

$$J_\theta \approx \frac{e}{c}\psi_t, \tag{A8}$$

https://doi.org/10.1017/S0022377822001039 Published online by Cambridge University Press

where $\psi_t = B_0 r^2/2$ and $\psi_p = \psi_t/q$ (here we neglect the magnetic shear) are the poloidal and toroidal magnetic fluxes, respectively, and (A4)–(A6), we obtain

$$\dot{r} = \frac{\hat{f}_\vartheta}{M\omega_B} = \frac{Rk_{\vartheta,s}}{M\omega_B\omega}\hat{P}_\alpha, \tag{A9}$$

$$\dot{v}_\parallel = \frac{1}{MR}\left(\dot{J}_\phi + \frac{1}{q}\dot{J}_\theta\right) = \frac{\hat{f}_\parallel}{M} = \frac{k_{\parallel,s}}{M\omega}\hat{P}_\alpha. \tag{A10}$$

One can see that after summation over particles these equations recover the ratio of the radial particle flux to the particle energy change, which follows from (3.22).

Appendix B. Derivation of equations for plasma rotation in the absence of collisions

In this appendix we derive equations describing the plasma reaction to external forces on short time intervals (when collisional effects are negligible), which we use in § 4. The derivation is based on the approach described in Hirshman (1978), Rosenbluth & Hinton (1996) and Helander & Sigmar (2005).

We are interested in the processes with characteristic times much longer than the particle transit time but much shorter than the collisional transport time. We therefore assume that all plasma parameters except for the flow velocities and the electric field are constant in time ($\partial/\partial t = 0$), the plasma flow of each plasma species σ is divergence-free,

$$\nabla \cdot (n_\sigma V_\sigma) = 0, \tag{B1}$$

and the radial flow is negligible. Then the general form of the plasma flow of each species is (Helander & Sigmar 2005)

$$\boldsymbol{V}_\sigma = \omega_\sigma(\psi_p)R\boldsymbol{e}_\varphi + \zeta_\sigma(\psi_p)\boldsymbol{B}, \tag{B2}$$

where

$$\omega_\sigma = -c\left(\frac{\partial \Phi}{\partial \psi_p} + \frac{1}{e_\sigma n_\sigma}\frac{\partial p_\sigma}{\partial \psi_p}\right), \tag{B3}$$

ψ_p is the poloidal magnetic flux, and $\zeta_\sigma(\psi_p)$ is arbitrary. It follows from (B2) that the poloidal rotation velocity is determined by ζ_σ; the binormal rotation velocity, by ω_σ; the toroidal one, by both. Differentiating (B3) with respect to time, we see that the binormal acceleration is the same for all the species, being associated with a corresponding change of the radial electric field:

$$\frac{\partial \omega_\sigma}{\partial t} = -c\frac{\partial \Phi'}{\partial t} \tag{B4}$$

with $\Phi' = \partial\Phi/\partial\psi_p$.

Following Hirshman (1978), Rosenbluth & Hinton (1996) and Helander & Sigmar (2005), we write

$$M_\sigma n_\sigma \frac{\partial}{\partial t}\left\langle BV_{\sigma\parallel}\right\rangle = \left\langle Bf_{\sigma\parallel}\right\rangle, \tag{B5}$$

$$M_\sigma n_\sigma \frac{\partial}{\partial t}\left\langle RV_{\sigma\varphi}\right\rangle = \frac{1}{c}\left\langle \boldsymbol{j}_\sigma \cdot \nabla\psi_p\right\rangle + \left\langle Rf_{\sigma\varphi}\right\rangle, \tag{B6}$$

where

$$\langle(\dots)\rangle = \oint \frac{\mathrm{d}\vartheta}{\boldsymbol{B}\cdot\nabla\vartheta}(\dots)\Big/\oint \frac{\mathrm{d}\vartheta}{\boldsymbol{B}\cdot\nabla\vartheta} \tag{B7}$$

https://doi.org/10.1017/S0022377822001039 Published online by Cambridge University Press

is flux-surface averaging. Our aim is to derive equations for the evolution of ω_σ and ζ_σ in terms of external forces applied to plasma species.

Averaging the longitudinal and toroidal projections of (B2) in an appropriate manner, we express ω_σ and ζ_σ in terms of quantities entering (B5) and (B6),

$$\zeta_\sigma = \frac{1}{\langle B_p^2\rangle \mathcal{K}}\left(\langle BV_{\sigma\parallel}\rangle - \frac{I^2}{\langle R^2\rangle}\langle RV_{\sigma\varphi}\rangle\right), \tag{B8}$$

$$\omega_\sigma = \frac{\langle B^2\rangle}{\langle B_p^2\rangle \mathcal{K}\langle R^2\rangle}\left(\langle RV_{\sigma\varphi}\rangle - \frac{I}{\langle B^2\rangle}\langle BV_{\sigma\parallel}\rangle\right), \tag{B9}$$

where $I = I(\psi_p) = B_\varphi R$, $\mathcal{K} = 1 + 2\hat{q}^2$,

$$\hat{q}^2 = \frac{I^2}{2\langle B_p^2\rangle}\left\langle \frac{1}{R^2} - \frac{1}{\langle R^2\rangle}\right\rangle, \tag{B10}$$

$\hat{q}^2 \approx q^2$ in a circular high-aspect-ratio tokamak.

From now on, we take $\boldsymbol{f}_\sigma \approx \boldsymbol{f}_\sigma^w$, disregarding all collisional processes. Combining (B5) and (B6) with (B8) and (B9), we obtain

$$M_\sigma n_\sigma \frac{\partial \omega_\sigma}{\partial t} = \frac{\langle B^2\rangle}{\langle B_p^2\rangle \mathcal{K}\langle R^2\rangle}\left(\frac{1}{c}\langle \boldsymbol{j}_\sigma \cdot \nabla\psi_p\rangle + \langle Rf_{\sigma\omega}\rangle\right), \tag{B11}$$

$$M_\sigma n_\sigma \frac{\partial \zeta_\sigma}{\partial t} = \frac{1}{\langle B_p^2\rangle \mathcal{K}}\left(-\frac{I}{c\langle R^2\rangle}\langle \boldsymbol{j}_\sigma \cdot \nabla\psi_p\rangle + \langle Bf_{\sigma u}\rangle\right), \tag{B12}$$

where

$$f_{\sigma\omega} = f_{\sigma\varphi} - \frac{I}{R\langle B^2\rangle}Bf_{\sigma\parallel}, \tag{B13}$$

$$f_{\sigma u} = f_{\sigma\parallel} - \frac{I}{B\langle R^2\rangle}Rf_{\sigma\varphi}. \tag{B14}$$

In a circular high-aspect-ratio tokamak

$$f_{\sigma\omega} \approx -f_{\sigma u} \approx -\frac{\epsilon}{q}f_{\sigma b} + 2\epsilon\cos\vartheta f_{\sigma\parallel}. \tag{B15}$$

Thus, approximately the same force projections determine the evolution of ω_σ and ζ_σ. As discussed in Helander & Sigmar (2005), the physical reason of the factor $\mathcal{K}$ appearing in (B11) and (B12) is that according to (B2), it is impossible to rotate plasma in the poloidal or binormal direction without involving toroidal rotation; the minimum possible energy of the toroidal motion is $2\hat{q}^2$ times larger than the energy of the poloidal motion.

https://doi.org/10.1017/S0022377822001039 Published online by Cambridge University Press

Next, we sum up (B11) for all species and use (B4) and

$$\frac{\partial \Phi'}{\partial t} = \frac{4\pi}{\left\langle B_p^2 R^2 \right\rangle} \sum_\sigma \left\langle \boldsymbol{j}_\sigma \cdot \nabla \psi_p \right\rangle . \tag{B16}$$

We arrive at

$$M_i n_i \frac{\partial \omega_i}{\partial t} = \frac{\left\langle B^2 \right\rangle}{(1+\lambda)\left\langle B_p^2 \right\rangle \mathcal{K} \left\langle R^2 \right\rangle} \sum_\sigma \langle R f_{\sigma\omega} \rangle \tag{B17}$$

where $\lambda \approx v_A^2/(\mathcal{K}c^2) \ll 1$ results from the contribution of the net current, and we have assumed that only the thermal ions contribute to the mass density.

Comparing (B11) and (B17), we find the radial currents,

$$\frac{1}{c}\left\langle \boldsymbol{j}_\sigma \cdot \nabla \psi_p \right\rangle = -\langle R f_{\sigma\omega} \rangle + \frac{M_\sigma n_\sigma}{(1+\lambda) M_i n_i} \langle R f_{\Sigma\omega} \rangle , \tag{B18}$$

$$\frac{1}{c}\sum_\sigma \left\langle \boldsymbol{j}_\sigma \cdot \nabla \psi_p \right\rangle = -\lambda \langle R f_{\Sigma\omega} \rangle , \tag{B19}$$

where $\boldsymbol{f}_\Sigma = \sum_\sigma \boldsymbol{f}_\sigma$. One can show that the radial currents of individual species almost cancel (the net current is approximately λ times the characteristic current of a single species). These currents redistribute the binormal force between species to provide their simultaneous acceleration according to (B4). Using (B11)–(B14) and (B18), we find that both toroidal and poloidal accelerations of all species are the same for all species when the longitudinal forces are absent,

$$\frac{\partial}{\partial t}\left\langle R V_{\sigma\varphi} \right\rangle = \frac{I}{M_\sigma n_\sigma \left\langle B^2 \right\rangle} \left\langle B f_{\sigma\parallel} \right\rangle + \frac{1}{M_i n_i} \langle R f_{\Sigma\omega} \rangle , \tag{B20}$$

$$\frac{\partial \zeta_\sigma}{\partial t} = \frac{1}{M_\sigma n_\sigma \left\langle B^2 \right\rangle} \left\langle B f_{\sigma\parallel} \right\rangle - \frac{I}{M_i n_i \left\langle B_p^2 \right\rangle \mathcal{K} \left\langle R^2 \right\rangle} \langle R f_{\Sigma\omega} \rangle . \tag{B21}$$

We conclude that the momentum provided by binormal and longitudinal forces are redistributed between plasma species in different manner. The binormal momentum is rapidly redistributed between the species by radial currents so that all species are accelerated simultaneously. The characteristic time of this redistribution is approximately the particle transit time (the time of relaxation of the velocity distribution to the form (B2) Helander & Sigmar (2005)). In contrast to this, there is no equally fast mechanism for the longitudinal momentum exchange between species. Therefore, this exchange takes place on much longer time scales determined by collisional or anomalous processes (friction between species, collisional stress, etc.).

Finally, averaging V_ϑ for high-aspect-ratio tokamak with circular cross-section, using (B2), (B13), (B4) and (B21) and keeping only leading-order terms, we obtain

$$\frac{\partial u_\vartheta}{\partial t} = \frac{c}{\langle B \rangle}\frac{\partial E_r}{\partial t} = \frac{f_{\Sigma\vartheta}}{M_i n_i \mathcal{K}} . \tag{B22}$$

REFERENCES

BELIKOV, V.S. & KOLESNICHENKO, YA.I. 1982 Derivation of the quasi-linear theory equations for the axisymmetric toroidal systems. *Plasma Phys.* **24** (1), 61.

https://doi.org/10.1017/S0022377822001039 Published online by Cambridge University Press

BELIKOV, V.S., KOLESNICHENKO, YA.I. & SILIVRA, O.A. 1992 Destabilization of the shear Alfvén mode by alpha particles and other high energy ions. *Nucl. Fusion* **32** (8), 1399.

BELOVA, E.V., GORELENKOV, N.N., CROCKER, N.A., LESTZ, J.B., FREDRICKSON, E.D., TANG, S. & TRITZ, K. 2017 Nonlinear simulations of beam-driven compressional Alfvén eigenmodes in NSTX. *Phys. Plasmas* **24**, 042505.

CHEN, L. & ZONCA, F. 2016 Physics of Alfvén waves and energetic particles in burning plasmas. *Rev. Mod. Phys*. **88** (1), 015008.

DING, S., GAROFALO, A.M., KNOLKER, M., MARINONI, A., MCCLENAGHAN, J. & GRIERSON, B.A. 2020 On the very high energy confinement observed in super H-mode DIII-D experiments. *Nucl. Fusion* **60** (3), 034001.

FUKAI, J. & HARRIS, E.G. 1971 Plasmons and the linear and nonlinear two-stream instabilities. *Phys. Fluids* **14** (8), 1748–1752.

GORELENKOV, N.N., PINCHES, S.D. & TOI, K. 2014 Energetic particle physics in fusion research in preparation for burning plasma experiments. *Nucl. Fusion* **54** (12), 125001.

GORELENKOV, N.N., STUTMAN, D., TRITZ, K., BOOZER, A., DELGADO-APARICIO, L., FREDRICKSON, E., KAYE, S. & WHITE, R. 2010 Anomalous electron transport due to multiple high frequency beam ion driven Alfvén eigenmodes. *Nucl. Fusion* **50** (8), 084012.

GREEN, B.J., ITER INTERNATIONAL TEAM & PARTICIPANT TEAMS 2003 ITER: burning plasma physics experiment. *Plasma Phys. Control. Fusion* **45**, 687–706.

HELANDER, P. & SIGMAR, D.J. 2005 *Collisional Transport in Magnetized Plasmas*, vol. 4. Cambridge University Press.

HINTON, F.L. & ROSENBLUTH, M.N. 1999 Dynamics of axisymmetric and poloidal flows in tokamaks. *Plasma Phys. Control. Fusion* **41** (3A), A653–A662.

HIRSHMAN, S.P. 1978 The ambipolarity paradox in toroidal diffusion, revisited. *Nucl. Fusion* **18** (7), 917.

IDA, K. & RICE, J.E. 2014 Rotation and momentum transport in tokamaks and helical systems. *Nucl. Fusion* **54** (4), 045001.

KADOMTSEV, B.B. 1982 *Collective Phenomena in Plasmas*. Pergamon.

KAUFMAN, A.N. 1972 Quasilinear diffusion of an axisymmetric toroidal plasma. *Phys. Fluids* **15**, 1063–1069.

KIM, HYUN-TAE, SIPS, A.C.C., ROMANELLI, M., CHALLIS, C.D., RIMINI, F., GARZOTTI, L., LERCHE, E., BUCHANAN, J., YUAN, X., KAYE, S. & JET CONTRIBUTORS. 2018 High fusion performance at high T_i/T_e in JET-ILW baseline plasmas with high NBI heating power and low gas puffing. *Nucl. Fusion* **58** (3), 036020.

KOLESNICHENKO, YA.I. 1980 The role of alpha particles in tokamak reactors. *Nucl. Fusion* **20** (6), 727.

KOLESNICHENKO, YA.I., KÖNIES, A., LUTSENKO, V.V. & YAKOVENKO, YU.V. 2011 Affinity and difference between energetic-ion-driven instabilities in 2D and 3D toroidal systems. *Plasma Phys. Control. Fusion* **53** (2), 024007.

KOLESNICHENKO, YA.I., LUTSENKO, V.V., TYSHCHENKO, M.H., WEISEN, H., YAKOVENKO, YU.V. & JET CONTRIBUTORS 2018 Analysis of possible improvement of the plasma performance in JET due to the inward spatial channelling of fast-ion energy. *Nucl. Fusion* **58** (7), 076012.

KOLESNICHENKO, YA.I., LUTSENKO, V.V., WOBIG, H. & YAKOVENKO, YU.V. 2002 Alfvén instabilities driven by circulating ions in optimized stellarators and their possible consequences in a Helias reactor. *Phys. Plasmas* **9**, 517.

KOLESNICHENKO, YA.I. & TYKHYY, A.V. 2018 Radial energy flux during destabilized Alfvén eigenmodes. *Phys. Plasmas* **25** (10), 102507.

KOLESNICHENKO, YA.I., TYKHYY, A.V. & WHITE, R.B. 2020 Spatial channeling in toroidal plasmas: overview and new results. *Nucl. Fusion* **60** (11), 112006.

KOLESNICHENKO, YA.I., YAKOVENKO, YU.V. & LUTSENKO, V.V. 2010*a* Channeling of the energy and momentum during energetic-ion-driven instabilities in fusion plasmas. *Phys. Rev. Lett*. **104**, 075001.

KOLESNICHENKO, YA.I., YAKOVENKO, YU.V., LUTSENKO, V.V., WELLER, A. & WHITE, R.B. 2010*b* Effects of energetic-ion-driven instabilities on plasma heating, transport and rotation in toroidal systems. *Nucl. Fusion* **50** (8), 084011.

KOLESNICHENKO, YA.I., YAMAMOTO, S., YAMAZAKI, K., LUTSENKO, V.V., NAKAJIMA, N., NARUSHIMA, Y., TOI, K. & YAKOVENKO, YU.V. 2004 Interplay of energetic ions and Alfvén modes in helical plasmas. *Phys. Plasmas* **11**, 158–170.

MORRIS, R.C., HAINES, M.G. & HASTIE, R.J. 1996 The neoclassical theory of poloidal flow damping in a tokamak. *Phys. Plasmas* **3**, 4513–4520.

PINCHES, S.D., CHAPMAN, I.T., LAUBER, PH.W., OLIVER, H.J.C., SHARAPOV, S.E., SHINOHARA, K. & TANI, K. 2015 Energetic ions in ITER plasmas. *Phys. Plasmas* **22** (2), 021807.

ROSENBLUTH, M.N. & HINTON, F.L. 1996 Plasma rotation driven by alpha particles in a tokamak reactor. *Nucl. Fusion* **36** (1), 55–67.

SAGDEEV, R.Z. & GALEEV, A.A. 1969 *Nonlinear Plasma Theory*. W.A. Benjamin, Inc.

SCOTT, S.D., DIAMOND, P.H., FONCK, R.J., GOLDSTON, R.J., HOWELL, R.B., JAEHNIG ,K.P., SCHILLING, G., SYNAKOWSKI, E.J., ZARNSTORFF, M.C., BUSH, C.E., *et al.* 1990 Local measurements of correlated momentum and heat transport in the TFTR tokamak. *Phys. Rev. Lett*. **64** (5), 531–534.

SIENA, A. DI, BILATO, R., GÖRLER, T., NAVARRO, A.B., POLI, E., BOBKOV, V., JAREMA, D., FABLE, E., ANGIONI, C., KAZAKOV, YE.O., *et al.* 2021 New high-confinement regime with fast ions in the core of fusion plasmas. *Phys. Rev. Lett*. **127**, 025002.

STUTMAN, D., DELGADO-APARICIO, L., GORELENKOV, N., FINKENTHAL, M., FREDRICKSON, E., KAYE, S., MAZZUCATO, E. & TRITZ, K. 2009 Correlation between electron transport and shear Alfvén activity in the National Spherical Torus Experiment. *Phys. Rev. Lett*. **102**, 115002.

THOMAS, P., GIROUD, C., LOMAS, P., STUBBERFIELD, P., RIMINI, F., TESTA, D., ZASTROW, K.-D. & DTE1 EXPERIMENTAL TEAM 2001 Alpha Heating of Thermal Ions in JET. *Proc. 28th EPS Conference on Contr. Fusion and Plasma Phys. (Funchal) Eur. Conf. Abstr.* **25A**, 929–932.

THOMAS, P.R., ANDREW, P., BALET, B., BARTLETT, D., BULL, J., DE ESCH, B., GIBSON, A., GOWERS, C., GUO, H., HUYSMANS, G., *et al.* 1998 Observation of alpha heating in JET DT plasmas. *Phys. Rev. Lett*. **80**, 5548.

TODO, Y. 2019 Introduction to the interaction between energetic particles and Alfvén eigenmodes in toroidal plasmas. *Rev. Mod. Plasma Phys*. **3**, 1.

TODO, Y., BERK, H.L. & BREIZMAN, B.N. 2010 Nonlinear magnetohydrodynamic effects on Alfvén eigenmode evolution and zonal flow generation. *Nucl. Fusion* **50** (8), 084016.

TSYTOVICH, V.N. 1977 *Theory of Turbulent Plasma*. Springer.

DE VRIES, P.C., VERSLOOT, T.W., SALMI, A., HUA, M.-D., HOWELL, D.H., GIROUD, C., PARAIL, V., SAIBENE, G., TALA, T. & JET-EFDA CONTRIBUTORS 2010 Momentum transport studies in JET H-mode discharges with an enhanced toroidal field ripple. *Plasma Phys. Control. Fusion* **52** (6), 065004.

WEISEN, H., CAMENEN, Y., SALMI, A., VERSLOOT, T.W., DE VRIES, P.C., MASLOV, M., TALA, T., BEURSKENS, M., GIROUD, C. & JET-EFDA CONTRIBUTORS 2012 Identification of the ubiquitous Coriolis momentum pinch in JET tokamak plasmas. *Nucl. Fusion* **52** (4), 042001.

WEISEN, H., SIPS, A.C.C., CHALLIS, C.D., ERIKSSON, L.-G., SHARAPOV, S.E., BATISTONI, P., HORTON, L.D., ZASTROW, K.-D. & EFDA-JET CONTRIBUTORS 2014 The scientific case for a JET D-T experiment. *AIP Conf. Proc*. **1612** (1), 77–86.

https://doi.org/10.1017/S0022377822001039 Published online by Cambridge University Press